Technical Note

An analytical approach to the conduction-dominated solidification of binary mixtures

J.D. Chung[a], J.S. Lee[a],*, S.T. Ro[a], H. Yoo[b]

[a] *Department of Mechanical Engineering, Seoul National University, Seoul 151-742, Korea*
[b] *Department of Mechanical Engineering, Soong Sil University, Seoul 156-743, Korea*

Nomenclature

c: specific heat
C: solute concentration
$\bar{C}_s$: average solute concentration in the solid phase
f_e: eutectic fraction at the solidus
f_s: solid fraction in the mushy region
h: enthalpy
k: thermal conductivity
L: latent heat of fusion
t: time
T: temperature
x: coordinate.

Greek symbols
α: thermal diffusivity
δ: position of phase interface
η: similarity variable
λ: similarity constant $(=\delta/\sqrt{4\alpha_l t})$
ρ: density
ω: position correction of phase interface.

Subscripts
e: eutectic
l: liquid
L: liquidus
m: mush
n: new value
o: old value
s: solid
S: solidus
w: wall

0: initial condition.

Superscript
*   ratio of the solid-to-liquid property.

1. Introduction

Analytical solutions are important for the model verification of models of solidification processes, particularly those involving binary mixtures where analytical or numerical solutions are difficult to obtain. A review of previous analytical studies shows that their approaches in the solid and liquid regions are somewhat straightforward and similar to each other. In the mushy region, however, different degrees of simplification are assumed on property and solid fraction, and the validity of those assumptions are not clearly evaluated. The assumptions made in the previous studies are summarized in Table 1.

In the present study, an analytical solution is obtained which is capable of the cooling condition below the eutectic temperature, and of microscopic effect in the evaluation of the solid fraction. The properties in the mushy region are weighted according to the solid fraction determined from the phase diagram. The aqueous ammonium chloride solution (NH_4Cl–H_2O) and aluminium copper alloy (Al–Cu) have been chosen as test binary systems because they are widely used as model systems in dendrite solidification studies, and their thermophysical properties are well established.

2. Analysis

A schematic of the physical model is depicted in Fig. 1. For simplicity, assumptions invoked in the analysis are as follows:

---

* Corresponding author. Tel.: 00 28 2 880 7117; fax: 00 82 2 883 0179; e-mail: jslee@gong.snu.ac.kr

Table 1
Summary of representative analytical studies and their assumptions

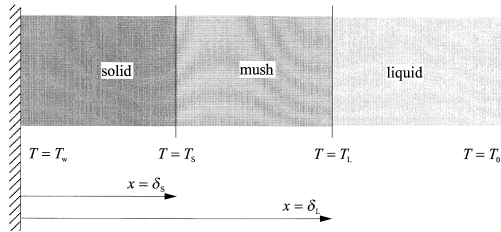|	Property assumption		Solid fraction assumption			Cooling condition	
	Constant	Variable	Length	Temp.	Phase diagram	$T > T_e$	$T < T_e$
Tien and Geiger [1]	O		O				O
Cho and Sunderland [2]	O		O				O
Muehlbauer et al. [3]	O						O
Özisik and Uzzell [4]	O		O	O			O
Kim and Kaviany [5]	O			O			O
Worster [6]		O				O	
Braga and Viskanta [7]		O			O	O	
Present		O			O		O

Fig. 1. Schematic diagram of the one-dimensional conduction-dominated solidification of a binary mixture.

1. The process is conduction-dominated.
2. All the thermophysical properties are constant within each phase. Density is assumed uniform throughout the phases.
3. Macroscopic species diffusion is negligible compared to thermal diffusion.

With the above assumptions, model equations describing temperature distributions in each region can be written as

$$\rho c_s \frac{\partial T}{\partial t} = k_s \frac{\partial^2 T}{\partial x^2}, \quad 0 < x < \delta_S \tag{1}$$

$$\frac{\partial}{\partial t}(\rho h_m) = \frac{\partial}{\partial x}\left(k_m \frac{\partial T}{\partial x}\right), \quad \delta_S < x < \delta_L \tag{2}$$

$$\rho c_l \frac{\partial T}{\partial t} = k_l \frac{\partial^2 T}{\partial x^2}, \quad \delta_L < x < \infty. \tag{3}$$

Initial conditions and boundary temperatures are self-evident. The heat flux conditions on the solidus and liquidus are

$$k_s \left(\frac{\partial T}{\partial x}\right)_- - k_m \left(\frac{\partial T}{\partial x}\right)_+ = \rho(h_m - h_s)\frac{d\delta_S}{dt}$$

$$= \rho(1 - f_e)\{(c_l - c_s)T_S + L\}\frac{d\delta_S}{dt}, \quad \text{at } x = \delta_S$$

$$k_m \left(\frac{\partial T}{\partial x}\right)_- - k_l \left(\frac{\partial T}{\partial x}\right)_+ = 0, \quad \text{at } x = \delta_L. \tag{5}$$

The weighted-averaged conductivity is evaluated considering the local solid fraction in the mushy region as follows:

$$k_m = f_s k_s + (1 - f_s)k_l \tag{6}$$

where the local solid fraction can be determined from the solutal mass balance equation given by

$$f_s = \frac{C_l(T) - C_0}{C_l(T) - \bar{C}_s} \tag{7}$$

where $\bar{C}_s$ is the average solute concentration in the solid phase. In this study, two limiting cases are considered. The first is known as lever rule which assumes no solutal concentration gradient in the solid, and the second is known as Scheil equation which assumes no mass diffusion in the solid.

Solutions in the solid and liquid regions can easily be obtained as functions of the well known similarity variable, $\eta \ (= x/\sqrt{4\alpha_l t})$, as follows:

$$\frac{T - T_w}{T_S - T_w} = \frac{\text{erf}(\sqrt{\alpha_l/\alpha_s}\eta)}{\text{erf}(\sqrt{\alpha_l/\alpha_s}\lambda_S)}, \quad 0 < \eta < \lambda_S \tag{8}$$

$$\frac{T - T_0}{T_L - T_0} = \frac{\text{erfc}(\eta)}{\text{erfc}(\lambda_L)}, \quad \lambda_L < \eta < \infty. \tag{9}$$

Unlike in the solid and liquid regions, the temperature profile in the mushy region can not be obtained in a

closed-form but can be expressed in the form of the second order ordinary differential equation as given below.

$$2\eta\left[f_s(c^*-1)+1+\left\{(c^*-1)T-\frac{L}{c_l}\right\}\frac{df_s}{dT}\right]\frac{dT}{d\eta} \tag{10}$$

$$+(k^*-1)\left(\frac{dT}{d\eta}\right)^2\frac{df_s}{dT}+\{f_s(k^*-1)+1\}\frac{d^2T}{d\eta^2}=0,$$

$$\lambda_S<\eta<\lambda_L.$$

Using the temperature profiles in the solid and liquid regions, equations (8) and (9), the interface conditions, equations (4) and (5), can be expressed as follows:

$$\left(\frac{dT}{d\eta}\right)_{\eta=\lambda_S-}=\frac{k^*}{f_e(k^*-1)+1}\frac{2}{\sqrt{\pi\alpha^*}}\frac{T_S-T_w}{\mathrm{erf}(\lambda_S/\sqrt{\alpha^*})}e^{-\lambda_S^2/\alpha^*}$$

$$-\frac{2\{L-(c_s-c_l)T_e\}}{c_l}\frac{1}{f_e(k^*-1)+1}(1-f_e)\lambda_S \tag{11}$$

$$\left(\frac{dT}{d\eta}\right)_{\eta=\lambda_L+}=\frac{2}{\sqrt{\pi}}\frac{T_0-T_L}{\mathrm{erfc}(\lambda_L)}e^{-\lambda_L^2}. \tag{12}$$

To determine the positions of solidus and liquidus, simultaneous solution to equations (11) and (12) should be obtained.

Previous works assume that the properties in the mushy region are constant and the solid fraction varies linearly with temperature or length in order to get a closed-form temperature profile in the mushy region. With these assumptions, the interfacial heat fluxes, $(dT/d\eta)_{\eta=\lambda_S-}$ and $(dT/d\eta)_{\eta=\lambda_L+}$, can be expressed explicitly, and substituting these values into equations (11) and (12) leads to non-linear algebraic equations. The positions of interface can then be obtained from the simultaneous solution of the algebraic equations. This approach, however, is in general not possible when variable properties in the mushy region are taken into consideration, and/or the solid fraction is determined from the solutal balance equation, because the temperature profile in the mushy region can no longer be obtained in a closed-form [7]. Thus, the key point in the solution procedure is how to find the interfacial heat fluxes from equation (10) and how to efficiently determine the interface positions from equations (11) and (12).

The heat fluxes at the interface, $(dT/d\eta)_{\eta=\lambda_S-}$ and $(dT/d\eta)_{\eta=\lambda_L+}$, are determined numerically by discretizing equation (10), and interface positions, λ_S and λ_L, are corrected as follows:

$$\lambda_n=\lambda_o(1+\omega). \tag{13}$$

Substituting the interfacial heat fluxes and interface correction equations into equations (11) and (12), and expanding these equations in a Taylor series up to the

second term for the interface position correction, it follows that

$$\omega_S\left[\frac{2\lambda_{S,o}}{\sqrt{\pi\alpha^*}}e^{-\lambda_{S,o}^2/\alpha^*}\left\{\left(\frac{dT}{d\eta}\right)_{\eta=\lambda_{S,o}-}+Q\lambda_{S,o}\right\}\right.$$

$$\left.+Pe^{-\lambda_{S,o}^2/\alpha^*}\frac{2\lambda_{S,o}^2}{\alpha^*}+Q\lambda_{S,o}\,\mathrm{erf}\left(\frac{\lambda_{S,o}}{\sqrt{\alpha^*}}\right)\right]$$

$$=Pe^{-\lambda_{S,o}^2/\alpha^*}-\mathrm{erf}\left(\frac{\lambda_{S,o}}{\sqrt{\alpha^*}}\right)\left[\left(\frac{dT}{d\eta}\right)_{\eta=\lambda_{S,o}-}+Q\lambda_{S,o}\right] \tag{14}$$

$$\omega_{L,o}e^{-\lambda_{L,o}^2}\left[\frac{2\lambda_{L,o}}{\sqrt{\pi}}\left(\frac{dT}{d\eta}\right)_{\eta=\lambda_{L,o}+}-2R\lambda_{L,o}^2\right]$$

$$=\left(\frac{dT}{d\eta}\right)_{\eta=\lambda_{L,o}+}\mathrm{erfc}\left(\lambda_{L,o}\right)-Re^{-\lambda_{L,o}^2} \tag{15}$$

where P, Q, and R are defined as follows:

$$P=\frac{2k^*}{f_e(k^*-1)+1}\frac{(T_S-T_w)}{\sqrt{\pi\alpha^*}}$$

$$Q=\frac{2}{f_e(k^*-1)+1}\frac{\{L-(c_s-c_l)T_e\}}{c_l}(1-f_e)$$

$$R=\frac{2}{\sqrt{\pi}}(T_0-T_L).$$

In the above equations (14) and (15), ω_S and ω_L should go to zero when the exact interfacial positions are obtained.

The solution procedure is summarized as described below:

1. Guess the interface positions, λ_S and λ_L.
2. Calculate the temperature profile from equation (10) and then the heat fluxes at the interfaces, $(dT/d\eta)_{\eta=\lambda_S-}$ and $(dT/d\eta)_{\eta=\lambda_L+}$.
3. Find ω_S and ω_L from equations (14) and (15), and then correct the interface positions.
4. Repeat the above procedure until the corrected interface positions, λ_S and λ_L, fall in the convergence criterion.

It is checked that the above iterative procedure is efficiently converged regardless of the initially guessed interface position in a matter of seconds on a personal computer. The solution offers computational advantages over a full numerical solution of governing partial differential equation in that it only requires the numerical solution of ordinary differential equation. It should be noted here that by this analytical method the non-equilibrium solidification process (Scheil equation) can be handled with no additional treatment to the previous equilibrium solidification analysis using the lever rule.

3. Results and discussion

The validity of the present solution is confirmed by comparing with Cho and Sunderland's [2] results obtained under simplified conditions (constant properties and linear variation of solid fraction with length). The comparison shows relative errors of only 0.003 and 0.005% in solidus and liquidus positions, respectively.

The constant property assumption in the mushy region is examined quantitatively. Since previous works selected test materials which have little difference in properties between the solid and liquid phases, evaluation of variable property effect has not been made properly. Figure 2 clearly shows that the constant property assumption may cause serious error. For example, the liquidus position with the constant property assumption is considerably overpredicted relative to that with variable property by 76% ($\eta_L = 2.75$ and 1.56, respectively) because the properties of the solid are much different from those of the liquid ($k^* = 5.769$, $c^* = 0.576$).

The results obtained based on various assumptions on solid fraction are compared in Fig. 3. The discrepancy due to the assumption of linear variation of solid fraction with length is obvious. Note that it is merely because the initial concentration of NH_4Cl–H_2O system is chosen near the eutectic point ($C_0 = 70\%$) that the solution based on linear variation with temperature (dotted line) nearly coincides with that based on the phase diagram (solid line). This means that because only a small portion is solidified in the mushy, the effect of the solid fraction model may not be apparent. This fact is evidenced when the solution is obtained with the initial concentration chosen far from the eutectic point.

The effect of the two limiting microscopic models for Al–Cu is shown in Fig. 4. The results for NH_4Cl–H_2O system are not demonstrated because the partition coefficient, k_p, for NH_4Cl–H_2O is zero and the two microscopic models thus become identical.
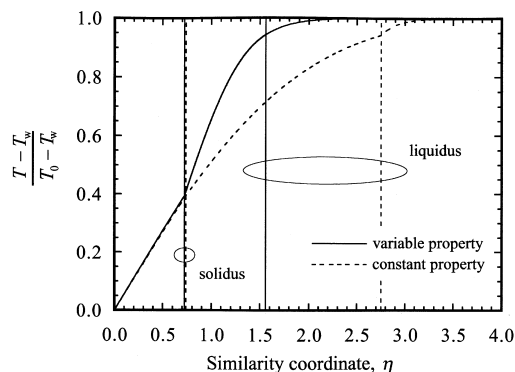

Fig. 2. The effect of variable mushy property weighted by the solid fraction from the phase diagram for NH_4Cl–H_2O ($C_0 = 70\%$).
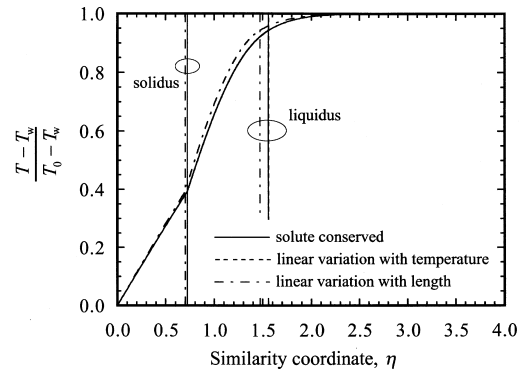

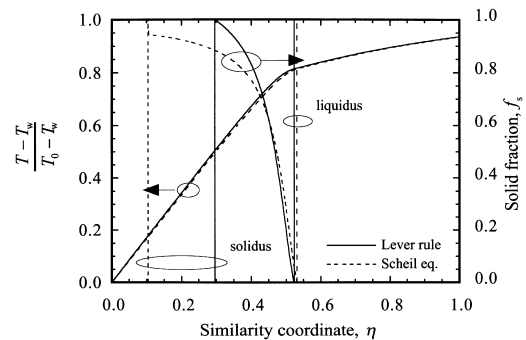Fig. 3. The effect of the solid fraction assumption for NH_4Cl–H_2O ($C_0 = 70\%$).

Fig. 4. The effect of microscopic models for Al–Cu with initial concentration, $C_0 = 3\%$.

4. Conclusions

Analytical and approximate solutions to the conduction-dominated solidification of binary mixtures are presented, which are distinct from previous works in the following aspects: (1) solid fraction is determined from the phase diagram; (2) thermophysical properties in the mushy region are weighted according to the local solid fraction; (3) non-equilibrium solidification can be simulated; and (4) the cooling condition of below-eutectic temperature can be accommodated.

The difficulty associated with determining unknown interface locations which is a key point of solution method is overcome by an efficient interface location updating algorithm.

References

[1] R.H. Tien, G.E. Geiger, A heat-transfer analysis of the solidification of a binary eutectic system, ASME J. Heat Transfer 80 (1967) 230–234.

[2] S.H. Cho, J.E. Sunderland, Heat-conduction problems with

melting or freezing, ASME J. Heat Transfer 91 (1969) 421–426.

[3] J.C. Muehlbauer, J.D. Hatcher, D.W. Lyons, J.E. Sunderland, Transient heat transfer analysis of alloy solidification, ASME J. Heat Transfer 95 (1973) 324–331.

[4] M.N. Özisik, J.C. Uzzell, Jr, Exact solution freezing in cylindrical symmetry with extended freezing temperature range, ASME J. Heat Transfer 101 (1979) 331–334

[5] C.J. Kim, M. Kaviany, A fully implicit method for diffusion-controlled solidification of binary alloys, Int. J. Heat Mass Transfer 35 (1992) 1143–1154.

[6] M.G. Worster, Solidification of an alloy from a cooled boundary, J. Fluid Mech. 167 (1986) 481–501.

[7] S.L. Braga, R. Viskanta, Solidification of a binary solution on a cold isothermal surface, Int. J. Heat Mass Transfer 33 (1990) 745–754.